Alias-free color Doppler with chirps

Pierre Ecarlat[1] Vincent Perrot[1] Ewen Carcreff[2]

Barbara Nicolas[1] Hervé Liebgott[1] Damien Garcia[1]

[1]CREATIS, CNRS, Inserm, UMR 5220, U1294, Lyon, France
[2]DB-SAS/TPAC, Nantes, France

***Abstract*—Ultrafast Doppler imaging is an increasingly used technique to quantify and visualize blood flow dynamics at a high frame rate. However, Doppler imaging is subject to phase wrapping (aliasing) when it comes to large velocities. Blood velocities are bounded by the Nyquist velocity (maximum measurable speed), which depends on the pulse repetition frequency (PRF) and central frequency. Several solutions have been proposed to achieve alias-free Doppler images: 1) post-processing of the Doppler images, some of which are based on deep learning, 2) combination of multiple Doppler fields with different Nyquist velocities, generated using dual-PRF emissions, or dual-frequency Doppler measurements. This work aims to improve the latter by using chirps, which have the double advantage of providing wide frequency bands and giving a better spatial resolution by matched filtering. Our results showed a significant drop in the percentage of errors (up to 12% in double aliasing) when using chirps over standard windowed sine waves (WSW). Chirps are known to improve spatial resolution in beamforming; our results support their use for Doppler imaging, as they help mitigate velocity ambiguity due to aliasing.**

***Index Terms*—color Doppler, aliasing, dual-frequency, chirp**

I. Introduction

Ultrafast color Doppler imaging with transmits of wide wavefronts can achieve high frame rates. This is particularly useful for monitoring flows with large temporal accelerations, as this ultrafast modality substantially increases the image rate. The speeds measured by Doppler imaging, whether from focused, plane or divergent waves, are bounded by the Nyquist velocity. Whenever the blood speed projected on the ultrasound axis exceeds this limit, the corresponding Doppler velocity is wrapped. The Nyquist velocity is proportional to the PRF (pulse repetition frequency), and inversely proportional to the center frequency f_0 of the emitted pulses. As for PRF, it is limited by the depth of the tissues to be scanned. It results that color Doppler imaging is faced with a velocity/depth trade-off, which can be a limitation in echocardiography where high blood velocities appear in deep sites, for example in the transmitral jet or in the ventricular outflow tract.

Several segmentation-based solutions have been proposed to remove aliasing in color Doppler images, by detecting aliased regions before unwrapping them. Some are based on standard image post-processing, such as region merging segmentation [1]. Recent works rely on CNN (convolutional neural network) deep learning [2] to pinpoint the aliased areas. These post-processing methods are dependent on the data and may fail in some situations. To overcome this problem, some approaches instead involve modifying the signal transmits. One strategy is to pair Doppler fields with different Nyquist velocities by using two or more interleaved transmits with different PRFs that are suitably chosen [3]. Each acquisition has a distinct aliasing pattern due to its own Nyquist velocity, and they can be combined to remove the Doppler ambiguity. Similarly, another way is to send successive pulses of different wavelengths, as proposed by Zrinc and Mahapatra [4] in Doppler radar. Following a similar approach for pulsed-wave Doppler, Nitzpon *et al.* [5] transmitted signals that contained two carrier frequencies. This method has the advantage of preserving the slow-time sampling rate as it does not require interleaved sequences. It was adapted by Porée *et al.* [6] who bandpass filtered wideband ultrasound signals instead of using two carrier frequencies.

On a different scope, it is known that coded excitations, combined with pulse compression, improve the signal-to-noise-ratio (SNR) of beamformed images [7]. Chirps have proven to be relevant for medical ultrasound imaging because they extend the frequency band of the excitation waveform, thus increasing the emitted energy and frequency information [8]. In the present work, we leveraged the wide spectral bandwidth of the chirps signals to improve the dual-frequency approach when eliminating aliasing in color Doppler. The received signals were processed with matched filtering to improve the axial resolution. Section 2 describes the theory of the dual-frequency approach, as well as the materials and metrics that were used to evaluate the performance of chirp-based color Doppler. The results on a flow phantom are shown in Section 3 and discussed in Section 4.

II. Methods and Materials

A. Dual-frequency dealiasing with chirps

Color Doppler imaging is governed by the Nyquist sampling rule, which states that the Doppler velocities are bounded on the interval $[-v_\mathrm{N}; v_\mathrm{N}]$, with v_N standing for the Nyquist velocity. When facing high speeds, the Doppler images are

P. Ecarlat, B. Nicolas, H. Liebgott and D. Garcia are with CREATIS (CNRS, Inserm, UMR 5220, U1294, Lyon, France). V. Perrot was with CREATIS. He is with Provost Ultrasound Lab (Montréal, Canada). E. Carcreff is with DB-SAS/TPAC (Nantes, France).
E-mail: pierre.ecarlat@creatis.insa-lyon.fr

aliased, which may lead to ambiguities in the flow analysis. The Doppler velocity v_{D} is related to the true (unambiguous) velocity v_{D}^{u} by $v_{\mathrm{D}}^{u} = v_{\mathrm{D}} + 2n_{\mathrm{N}}v_{\mathrm{N}}$, where the integer n_{N} is termed the Nyquist number. Solving the aliasing problem consists in determining the Nyquist number of each pixel. In a dual-frequency scheme, the signals, centered at f_{0_1} and f_{0_2} respectively, lead to two Doppler velocities:

$$\begin{cases} v_{\mathrm{D}}^{u} = v_{\mathrm{D}_1} + 2n_{\mathrm{N}_1}v_{\mathrm{N}_1} \\ v_{\mathrm{D}}^{u} = v_{\mathrm{D}_2} + 2n_{\mathrm{N}_2}v_{\mathrm{N}_2} \end{cases} \tag{1}$$

In this configuration, two Nyquist numbers, n_{N_1} and n_{N_2}, must be determined in a pixel-wise manner. To solve Equation (1), the center frequencies can be chosen such that [3]:

$$f_{0_1} = \frac{p}{q} f_{0_2} \tag{2}$$

with $p \in \mathbb{Z}^{+}$ and $q = p + 1$. For this dual-frequency scheme, the new (unambiguous) Nyquist velocity [3], [9] is equal to p times the Nyquist velocity associated with the lowest central frequency ($v_{\mathrm{N}}^{u} = p \times v_{\mathrm{N}_1}$). It can be shown [3] that the Doppler velocities are related to the Nyquist numbers by:

$$\mathrm{nint}\left(q\frac{v_{\mathrm{D}_2} - v_{\mathrm{D}_1}}{2v_{\mathrm{N}_1}}\right) = q.n_{\mathrm{N}_1} - p.n_{\mathrm{N}_2} \tag{3}$$

where nint is the nearest integer function. For natural numbers p and q that are correctly chosen (we used $q = p + 1$), this equation can return n_{N_1} and n_{N_2}. As demonstrated in [3], the two Nyquist numbers are constrained by the following inequalities:

$$\begin{aligned} |n_{\mathrm{N}_1}| &\leq \mathrm{ceil}\left(\frac{p}{2} - \frac{1}{2}\right) \\ |n_{\mathrm{N}_2}| &\leq \mathrm{ceil}\left(\frac{q}{2} - \frac{1}{2}\right) \\ |n_{\mathrm{N}_1}q - n_{\mathrm{N}_2}p| &\leq \frac{1}{2}(p+q) \end{aligned} \tag{4}$$

Given these constraints, the number of possible couples $\{n_{\mathrm{N}_1}, n_{\mathrm{N}_2}\}$ that are solutions of Equation (3) is $2p + 1$ when $q = p+1$. A small lookup table can thus be built to determine the Nyquist numbers. Table I of [3] is an example with $p = 3$ and $q = p + 1 = 4$. Once the Nyquist numbers are known, one or the other expression of the system (1) can be chosen to obtain the unambiguous Doppler values. To decrease Doppler variance, it is advisable to calculate a weighted mean:

$$v_{\mathrm{D}}^{u} = \frac{p}{p+q}\left(v_{\mathrm{D}_1} + \frac{q}{p}v_{\mathrm{D}_2} + 2v_{\mathrm{N}_1}(n_{\mathrm{N}_1} + n_{\mathrm{N}_2})\right) \tag{5}$$

B. Pulse waveform and chirp compression

We compared two types of pulse: standard windowed sine waves (WSW) and linear up-chirps. The former was a simple subset of a sinusoidal signal, oscillating at f_0, and was used as a reference to evaluate the effectiveness of chirps. Before windowing, they can be written as:

$$\Psi_{\mathrm{wsw}}(t) = \sin(2\pi f_0 t) \tag{6}$$

while chirps have a linear frequency modulation:

$$\Psi_{\mathrm{chirp}}(t) = \sin\left(2\pi f_1 t + \pi\left(\frac{f_2 - f_1}{T}\right)t^2\right) \tag{7}$$

with T the time (in s) it takes to sweep from f_1 to f_2. Note that chirps are, in essence, long-duration pulses. A chirp compression process by matched filter is thus required to recover a narrow pulse of increased amplitude. In this study, we correlated the received signals with a template of the emitted chirp. Figure 1 compares the spectra of the windowed-sine and chirp signals, before and after band-pass filtering. Because of their longer duration, chirp pulses transport more acoustic energy. Therefore, chirps should be more efficient for dual-frequency color Doppler. We tested this hypothesis in an *in vitro* Poiseuille flow setup.

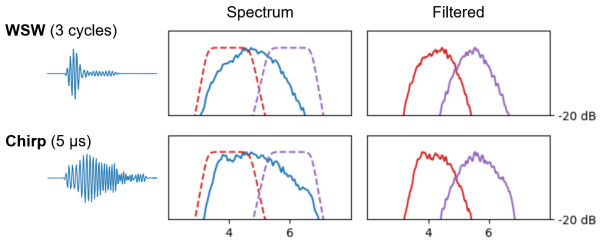

Fig. 1. Effect of filters on beamformed data for WSW (top row) and chirps (bottom row). From left to right: 1) the transmitted pulse, 2) the spectrum of the beamformed data in blue, and the band-pass filters to apply, 3) the filtered low and high-frequency spectra.

C. Materials and in vitro experiments

RF signals were acquired with the OEMPA2 ultrasound scanner (The Phased Array Company - TPAC, Nantes, France) and a 5.2 MHz linear probe (ATL-L7-4, Philips, 128 elements, pitch = 300 μm, 3-to-7 MHz bandwidth). Plane waves were transmitted with a 0° steering angle. Experiments were made on a 40° slanted vessel (Doppler 403 Flow phantom). Both windowed-sine and linear up-chirp pulses were generated using the provided Arbitrary Waveform Generation tool of TPAC. The chirp-based RF signals were matched filtered using a template signal. The signals were I/Q demodulated and beamformed [10] on GPU. The center frequencies of the band-pass filters were set at 4 and 6 MHz (in respect with equation (2), with $p = 2$ and $q = 3$). After a polynomial wall filtering, Doppler fields were computed with a pixel-wise autocorrelator and a packet size of 30. The real envelope was computed in the last frame of the packet to provide a B-Mode background image. The images contained 256×256 pixels of axial/lateral size 55×100 μm. Details are given in Table I.

TABLE I
SETTINGS FOR THE ACQUISITION AND DOPPLER COMPUTATION

Probe parameters		Doppler parameters	
Center frequency	5.2 MHz	Beamforming	DAS
Nb. of elements	128	Pixel size	55 ×100 μm
Pitch	300 μm	Packet size	30
Bandwidth	3-to-7 MHz	Wall filter	Quadratic
Sampling frequency	25 MHz	Smoothing	None

The ultrasound acquisitions were carried out on a Poiseuille (steady) flow of 2.5 mL/s at different PRF to produce a range of aliasing situations. Eight PRF were tested, ranging between 500 and 2000 Hz, which led to three different aliasing schemes: 1) no aliasing, 2) single aliasing with different Nyquist limits, and 3) double aliasing. For quantitative analyses, we selected a region of interest (ROI) from the vessel lumen in the center of the scan area. Knowing the actual *in vitro* velocity profiles, we defined dealiasing errors as the number of uncorrected or incorrectly corrected pixels relative to the number of pixels in the ROI (in %). We averaged the results over 20 Doppler fields.

D. Configurations of the transmit signals

1) Number of cycles for the WSW: As stated in section II-B, the bandwidth of the pulse-echo signals should be wide enough to enable them to be filtered in both the low and high frequency components. Using WSW, it is possible to achieve large bandwidths with short pulses, for example one to two cycles (wavelengths) (Fig. 2b). Short pulses, however, produce low-SNR Doppler signals and thus noisy color Doppler images (Figure 2c). As a consequence, a trade-off must be made between the transmitted energy and the spectral bandwidth.

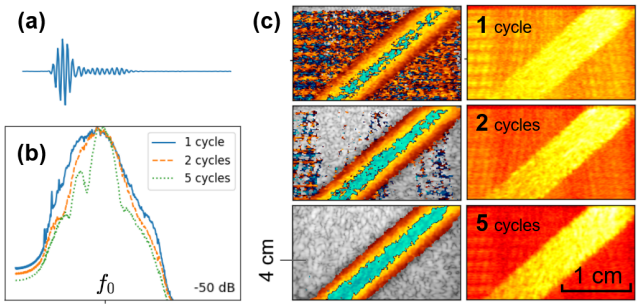

Fig. 2. WSW characteristics: a) an example of emitted WSW, b) effect of cycle number on spectra, and c) effect of cycle number on color (left) and power (right) Doppler. A power threshold of -30 dB was applied on the color Doppler images.

To identify the optimal number of cycles for our experiments, we tested several pulses of different duration (from 1 to 6 cycles) on a single aliasing setup (PRF at 1000 Hz). The top row of table II shows that the lowest error was obtained with a WSW of two cycles. Given these results, the comparison against chirps was made with short pulses of two cycles.

2) Chirp duration: Similarly, we sought an optimal chirp duration, in the range of 1 to 10 μs. The bottom row of table II shows that chirp duration longer than 2 μs led to smaller errors. In this work, we thus generated chirps of 5 μs as they performed slightly better. Following these prior measurements, the effectiveness of the dual-frequency method for Nyquist velocity extension was tested with 2-cycle WSWs and 5-microsecond chirps under different aliasing settings.

III. Results

A. WSW vs. chirp for dual-frequency dealiasing

The first column of Figure 3 displays the Doppler velocities obtained with a standard Doppler method (one frequency, 5 MHz) for different PRF, while the flow rate remained unchanged (2.5 mL/s). The second and third column compares the unambiguous (alias-free) color Doppler obtained with the WSW and chirp signals, respectively. Dual-frequency dealiasing was successful (Fig. 3 and 4) with both pulse types (WSW and chirps) when aliasing was moderate (PRF of 1000 Hz). However, when aliasing became predominant (with decreasing PRF), the Doppler reconstruction errors became significant with WSW pulses (blue curve in Fig. 4). As for the chirp-based transmits, they remained effective in any condition of single aliasing (red curve in Fig. 4). The dealiasing errors were substantial for both pulse types (14% and 26%) in the double-aliasing scenario at low PRF (PRF = 500 Hz). That being said, the chirp pulses produced fewer dealiasing errors in all situations.

TABLE II
Dealiasing errors (in%) for WSW and chirp configurations

WSW (% of incorrect dealiasing per number of cycles)

nb	1	1.5	**2**	2.5	3	3.5	4	4.5	5	5.5	6
%	2.66	1.56	**0.64**	0.72	1	1.26	1.4	1.4	1.17	1	1.1

Chirp (% of incorrect dealiasing per signal duration, in μs)

μs	1	2	3	4	**5**	**6**	7	8	9	10
%	2.3	0.33	0.32	0.36	**0.17**	**0.17**	0.22	0.25	0.23	0.18

B. Smoothing with a kernel-based auto-correlation

In this study, we used a pixel-wise Doppler auto-correlator for comparison purposes. In color Doppler, it is nevertheless recommended to use a spatial kernel when auto-correlating, for less noisy estimates of the phase shift. To complete our study qualitatively, we tested a 11-by-11 median-filter kernel on the noisiest case. Figure 5 shows the effect of the median-filter kernel in the double-aliasing scenario, for both pulse types. The Doppler images show improvements in correcting isolated dealiasing errors, regardless of the pulse. However, in large noisy areas, such as those from the WSW, the kernel used in the auto-correlation failed to fix the errors, or even made them worse (blurring effect). Chirps, which generate more sparse errors, are more likely to benefit from a spatial kernel.

IV. Discussion and Conclusion

Our results show that the dual-frequency method for removing aliasing ambiguity had significant limitations with WSW pulses, even in single-aliasing scenarios. The dual-frequency dealiaser performed better with chirp pulses regardless of the aliasing situation. In addition, because incorrect pixels are more sparsely distributed with chirp pulses, they are more likely to be corrected by conventional kernel-based smoothing when auto-correlation the complex signals. Chirps are known to improve spatial resolution in ultrasound imaging [8]; our results suggest that they can also be used in Doppler imaging as they help mitigate velocity ambiguity due to aliasing.

Since the bandwidths of the WSW and chirp pulses after band-pass filtering are relatively similar, it is most likely that the improvement observed with chirps is related to the longer pulse duration. Doppler variance is indeed reduced

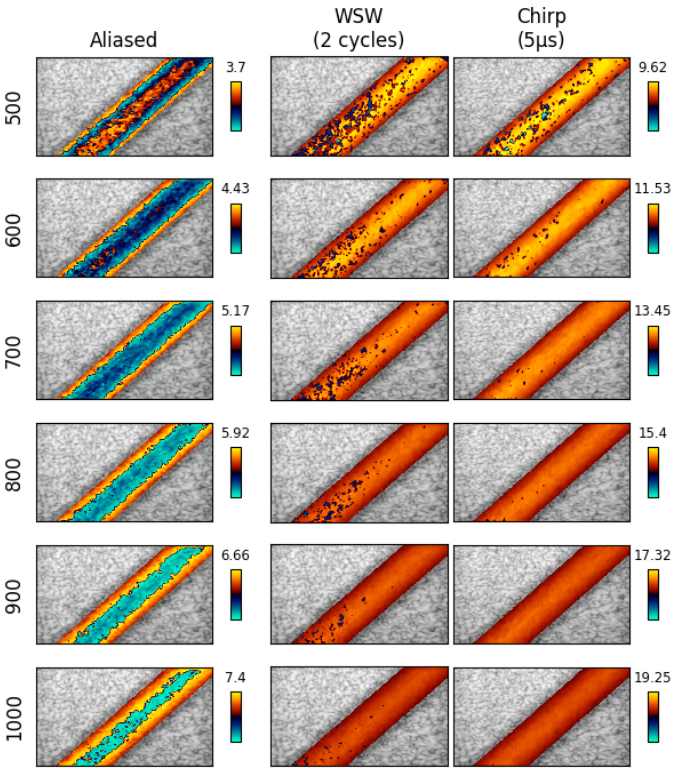

Fig. 3. Original color Doppler maps (first column), and their alias-free estimates for both pulse types (WSW and chirp). Each row presents a different aliasing situation, with a PRF increasing from 500 to 1000 Hz. The Doppler velocities are in cm/s.

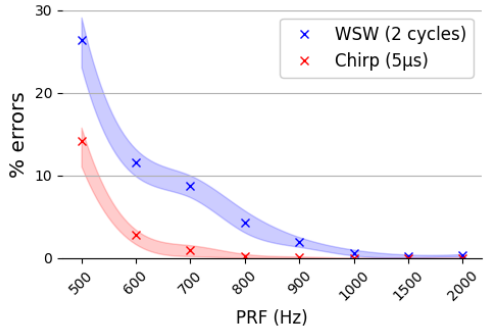

Fig. 4. Dealiasing errors for WSW and chirps with increasing PRFs. The shaded areas represent ± standard deviation over the 20 acquisitions.

when longer pulses are used, as suggested by the Cramér-Rao limit. [11]. Whether this Cramér-Rao bound still works in chirps should be verified. Further investigations should also be completed with a probe of wider spectral bandwidth to quantify its effect on dual-frequency dealiasing. Another consideration is the increased energy of the chirp. It leads to a better signal-to-noise ratio, and consequently to a better quality of B-Modes images [8]. Likewise, it probably decreases Doppler variance and thus improves the dealiasing method. On the other hand, the temperature increase due to the frequency modulation and the pulse duration can be the source of electronic issues when transmitting chirp pulses. In view of the known results and our findings, the benefit of chirps deserves to be addressed for medical ultrasound imaging.

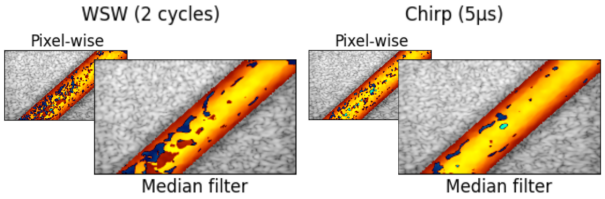

Fig. 5. Effect of a median-filter kernel on color Doppler, for both WSW and chirps.

V. Aknowledgments

This work was supported by the ANR-19-LCV2-0004-01 LabCom Image4US operated by the French National Research Agency (ANR). This work was supported by LABEX CELYA (ANR-10-LABX-0060) and the LABEX PRIMES (ANR-11-LABX-0063) of Université de Lyon, within the program "Investissements d'Avenir" (ANR- 11-IDEX-0007 and ANR-16-IDEX-0005), by the LabCom Image4US (ANR-19-LCV2-0004-01) operated by the French National Research Agency (ANR). This material is based upon work done on the PILoT facility (PILoT, INSA-Lyon).

References

[1] S. Muth, S. Dort, I. A. Sebag, M.-J. Blais, and D. Garcia, "Unsupervised dealiasing and denoising of color-Doppler data," *Medical image analysis*, vol. 15, no. 4, pp. 577–588, 2011.

[2] H. Nahas, J. S. Au, T. Ishii, B. Y. Yiu, A. J. Chee, and C. Alfred, "A deep learning approach to resolve aliasing artifacts in ultrasound color flow imaging," *IEEE Transactions on Ultrasonics, Ferroelectrics, and Frequency Control*, vol. 67, no. 12, pp. 2615–2628, 2020.

[3] D. Posada, J. Porée, A. Pellissier, B. Chayer, F. Tournoux, G. Cloutier, and D. Garcia, "Staggered multiple-PRF ultrafast color Doppler," *IEEE transactions on medical imaging*, vol. 35, no. 6, pp. 1510–1521, 2016.

[4] D. Zrinc and P. Mahapatra, "Two methods of ambiguity resolution in pulse Doppler weather radars," *IEEE Transactions on Aerospace and Electronic Systems*, no. 4, pp. 470–483, 1985.

[5] H. Nitzpon, J. Rajaonah, C. Burckhardt, B. Dousse, and J. Meister, "A new pulsed wave Doppler ultrasound system to measure blood velocities beyond the Nyquist limit," *IEEE transactions on ultrasonics, ferroelectrics, and frequency control*, vol. 42, no. 2, pp. 265–279, 1995.

[6] J. Porée, G. Goudot, O. Pedreira, E. Laborie, L. Khider, T. Mirault, E. Messas, P. Julia, J.-M. Alsac, M. Tanter *et al.*, "Dealiasing high-frame-rate color doppler using dual-wavelength processing," *IEEE Transactions on Ultrasonics, Ferroelectrics, and Frequency Control*, vol. 68, no. 6, pp. 2117–2128, 2021.

[7] M. O'Donnell, "Coded excitation system for improving the penetration of real-time phased-array imaging systems," *IEEE transactions on ultrasonics, ferroelectrics, and frequency control*, vol. 39, no. 3, pp. 341–351, 1992.

[8] S. Harput, J. McLaughlan, D. M. Cowell, and S. Freear, "Contrast-enhanced ultrasound imaging with chirps: Signal processing and pulse compression," in *2015 IEEE International Ultrasonics Symposium (IUS)*. IEEE, 2015, pp. 1–4.

[9] P. Tabary, F. Guibert, L. Perier, and J. Parent-du Chatelet, "An operational triple-PRT Doppler scheme for the French radar network," *Journal of Atmospheric and Oceanic Technology*, vol. 23, no. 12, pp. 1645–1656, 2006.

[10] V. Perrot, M. Polichetti, F. Varray, and D. Garcia, "So you think you can DAS? A viewpoint on delay-and-sum beamforming," *Ultrasonics*, no. 111, p. 106309, 2021.

[11] W. F. Walker and G. E. Trahey, "A fundamental limit on delay estimation using partially correlated speckle signals," *IEEE transactions on ultrasonics, ferroelectrics, and frequency control*, vol. 42, no. 2, pp. 301–308, 1995.